CHARGE EXCHANGE SCATTERING OF 1 GEV PROTONS BY NUCLEI

V.P.Koptev, E.M.Maev, M.M.Makarov, A.V.Khanzadeev

Introduction

Study of the neutron production in proton-nucleus interactions is important for understanding of the mechanism of these interactions and for investigation of the nuclear structure. But there were only few experiments (see Ref. [1] and references in it), and they were devoted mainly to the zero angle neutron emission. In most of the experiments, the information about the energy spectra of neutrons is obtained from the additional scattering of neutrons on the hydrogen target. In the present work, the neutron energy was measured by the time-of-flight method with the use of time microstructure of the proton beam [2]. The use of this method was possible due to appropriate time parameters of the proton beam from the PNPI synchrocyclotron, and this gave the opportunity to increase the statistics in comparison with the double scattering method. For the first time, systematic studies of the neutron production from many nuclei were done in the range of $1 \leq A \leq 208$ at several angles. The method and the setup are described in Ref. [1]. The double differential cross sections for neutron production from ^{11}B and ^{181}Ta are presented in Fig. 1. Similar spectra were measured for other nuclei. Two peaks are obviously seen in all the spectra. The peak in the region of higher energies is due to the process of quasielastic knockout. Its location (T_1) is slightly different from the value of the kinetic energy (T_2) corresponding to the kinematics of the proton-neutron elastic scattering.

The mean neutron separation energy $\Delta E = T_2 - T_1$ for different nuclei is presented in Fig. 2. The value of ΔE becomes constant for the nuclei heavier than carbon. The cross sections for the quasielastic knockout $(d\sigma/d\Omega)^{\rm ex}$ were obtained by integration of the energy spectra in the region of the quasielastic peak via the procedure described in Ref. [1], and had several features:

1. for the symmetric ($N = Z$) nuclei, $(d\sigma/d\Omega)^{\rm ex}$ is proportional to $A^{1/3}$;
2. for the nuclei heavier than Cu ($N > Z$), $(d\sigma/d\Omega)^{\rm ex}$ becomes proportional to $A^{2/3}$;
3. for all studied isotopes of B, Mg, Ca, and Sn, a considerable increase of the cross sections is found with the number of neutrons increasing.

The above mentioned features can be described within 10% accuracy by the simple phenomenological expression

$$d\sigma/d\Omega^{\rm ex} = C_{\rm ex}(\theta) \cdot N/Z \cdot A^{1/3},$$

with the normalization coefficients $C_{\rm ex}$ equal to 18.5, 14.8, and 10.5 mb/sr for the angles 4°, 7.5°, and 11.3°. The second wide peak in the energy spectra of neutrons is caused by the neutron production in inelastic reactions. The atomic number dependence of these inelastic cross sections is well approximated by the expression

$$d\sigma/d\Omega^{\rm in} = C_{\rm in}(\theta) \cdot A^{1/2},$$

with $C_{\rm in}(\theta)$ equal to 51.3, 36.8, and 25.1 mb/sr for the angles 4°, 7.5°, and 11.3°. For all the three angles the values of the coefficients $C_{\rm ex}(\theta)$ and $C_{\rm in}(\theta)$ appeared to be very close to the cross sections of the quasielastic and inelastic knockout of neutrons from deuterons, which were measured in this experiment.

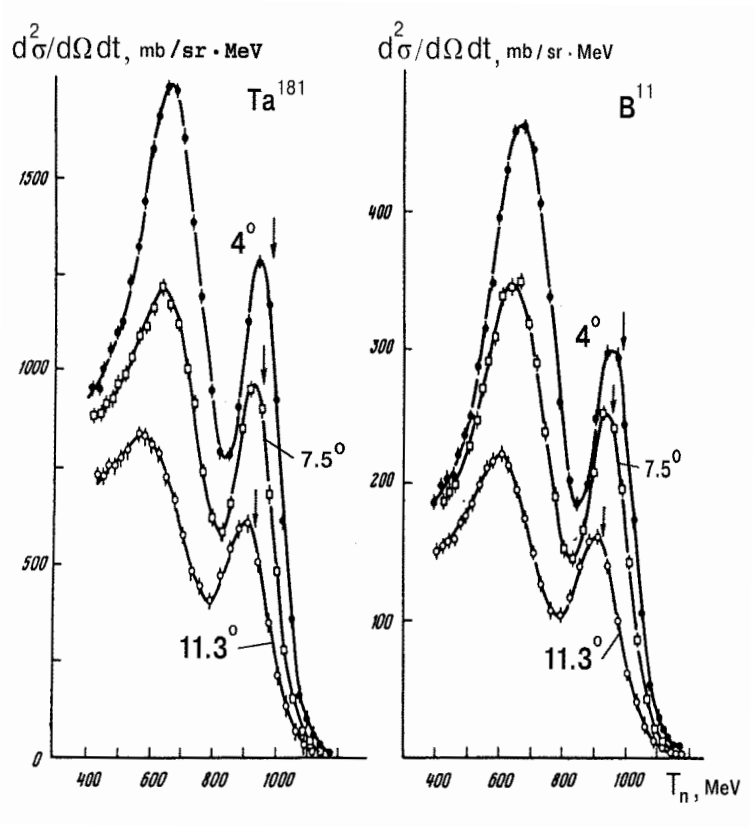

Fig. 1. Neutron spectra from ^{11}B and ^{181}Ta at angles 4°, 7.5°, and 11.3°. The arrows show the energy of neutrons corresponding to *pn* elastic scattering.

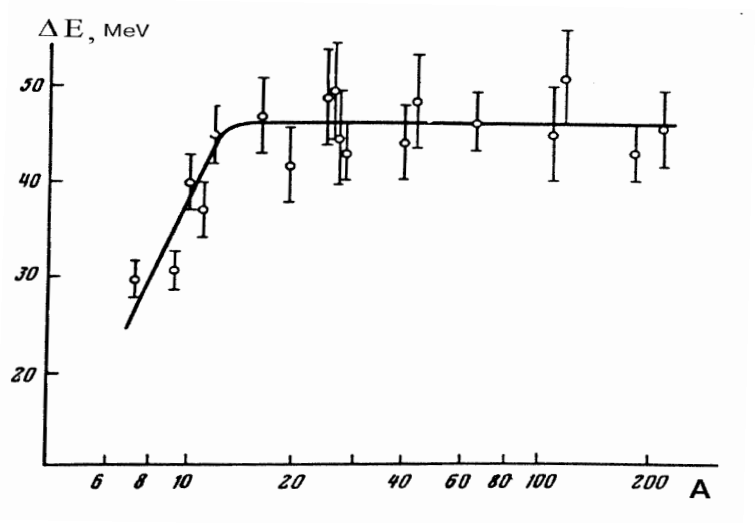

Fig. 2. Mean energy of neutron separation from nuclei in quasielastic knockout reaction. The curve has been drawn by hand.

The cross sections of the quasielastic neutron production were calculated in the frame of the Glauber theory [3].

Charge exchange scattering in the Glauber theory

Let us consider the charge exchange scattering of protons by nuclei:

$$p + {}^{Z}A_N \to n + {}^{Z+1}A_{N-1}. \tag{1}$$

If the state of the residual nucleus is not selected in the experiment, so that the cross section is summed up over all final states (the nucleus ${}^{Z+1}A_{N-1}$ may be in an excited state), the completeness condition tells us that the cross section for the reaction (1) is determined solely by the ground-state wave function of the nucleus and can be calculated on the base of the Glauber theory. In measurements of the neutron energy, the resolution of $\sim$100 MeV is sufficient to discriminate reliably against cases of the neutron production in meson-production reactions and at the same time to span a sufficiently large number of final nuclear states.

In the Glauber theory, the cross section for reaction (1) can be written as [3]:

$$\frac{d\sigma}{d\Omega} = \left(\frac{k}{2\pi}\right)^2 N \int d^2b\, d^2b' \exp(i\vec{q}(\vec{b}-\vec{b}'))H_o(\vec{b},\vec{b}') \times$$
$$\times\Big[1 - h_p(\vec{b}) - h^*(\vec{b}') + H_p(\vec{b},\vec{b}')\Big]^Z \Big[1 - h_n(\vec{b}) - h_n^*(\vec{b}') + H_n(\vec{b},\vec{b}')\Big]^{N-1}, \tag{2}$$

where

$$\begin{aligned}
h_{p,n}(\vec{b}) &= \int G_{el}(\vec{b}-\vec{s})\rho_{p,n}(\vec{r})d^3r, \\
H_{p,n}(\vec{b},\vec{b}') &= \int G_{el}(\vec{b}-\vec{s})G_{el}^*(\vec{b}'-\vec{s})\rho_{p,n}(\vec{r})d^3r, \\
H_o(\vec{b},\vec{b}') &= \int G_o(\vec{b}-\vec{s})G_o^*(\vec{b}'-\vec{s})\rho_n(\vec{r})d^3r, \\
G_{el,o}(\vec{b}) &= \frac{1}{2\pi i k}\int f_{el,o}(\vec{q})\exp(-i\vec{q}\vec{b})d^2q.
\end{aligned}$$

Here $\vec{q} = \vec{k} - \vec{k}_n$ is the momentum transfer ($t = -q^2$); $\vec{k}$ and $\vec{k}_n$ are the momenta of the incident proton and of the emitted neutron; $\vec{s}$ and $\vec{b}$ are the transverse coordinate of one of the nuclear nucleon and the impact-parameter vector, both lying in the plane perpendicular to $\vec{k}$; N and Z are the numbers of neutrons and protons in the nucleus; $f_{el}(\vec{q})$ is the amplitude of the nucleon-nucleon elastic scattering; $f_o(q)$ is the amplitude of the charge exchange reaction $pn \to np$; $\rho_{p,n}(r)$ is the one-particle proton or neutron density distribution.

If we adopt Gaussian parametrizations for the nucleon-nucleon amplitudes,

$$|f_{el}(\vec{q})|^2 = C\exp(-bq^2),$$
$$|f_o(\vec{q})|^2 = A_1\exp(-a_1q^2) + A_2\exp(-a_2q^2),$$

we find that (2) becomes

$$\frac{d\sigma}{d\Omega} = N_1 \mid f_o(q) \mid^2 + N_2\epsilon\left[\frac{bA_1}{b+a_1}\exp\left(\frac{ba_1}{b+a_1}t\right) + \frac{bA_2}{b+a_2}\exp\left(\frac{ba_2}{b+a_2}t\right)\right] +$$
$$+ \cdots + N_{m+1}\epsilon^m\left[\frac{bA_1}{b+ma_1}\exp\left(\frac{ba_1}{b+ma_1}t\right) + \frac{bA_2}{b+ma_2}\exp\left(\frac{ba_2}{b+ma_2}t\right)\right] + \cdots, \tag{3}$$

where

$$\epsilon = C/(\sigma_{\text{eff}}b); \qquad t = -q^2.$$

All the results discussed below were obtained using Eq. (3).

Calculated results

When calculating the differential cross section $d\sigma/d\Omega$ for reaction (1) we used the following data on nucleon-nucleon scattering at 1 GeV:

$$\begin{array}{lcllcl}
\sigma_{pp}^{tot} & = & 47.5\text{mb}, & \sigma_{pn}^{tot} & = & 38.2\text{mb}, \\
\alpha_{pp} & = & \dfrac{\text{Re}f_{el}^{pp}(0)}{\text{Im}f_{el}^{pp}(0)} = -0.1, & \alpha_{pn} & = & \dfrac{\text{Re}f_{el}^{pn}(0)}{\text{Im}f_{el}^{pn}(0)} = -0.4, \\
b & = & 6.5\,(\text{GeV/c})^{-2} \text{ (we assume that } b_{pp} = b_{pn}), & & & \\
C & = & \mid f_{el}(0) \mid^2 = \mid \dfrac{f_{el}^{pp}(0) + f_{el}^{pn}(0)}{2} \mid^2, & f_{el}^{pp,pn}(0) & = & \dfrac{ik}{4\pi}\sigma_{pp,pn}(1 - \alpha_{pp,pn}), \\
A_1 & = & 24.4 \text{ mb/sr}, & A_2 & = & 21.8 \text{ mb/sr}, \\
a_1 & = & 156.0\ (\text{GeV/c})^{-2}, & a_2 & = & 6.5\ (\text{GeV/c})^{-2}
\end{array}$$

(A_1, A_2, a_1, and a_2 are taken from the data of G.Bizard et al. (1975)).

For the nucleon density distribution for nuclei with $A \geq 19$, there was chosen a Fermi distribution with two parameters:

$$\rho_{p,n}(r) = \rho_{p,n}^0 \left[1 + \exp\left(\frac{r - R_{p,n}}{a_{p,n}}\right)\right]^{-1}, \tag{4}$$

where R is the radius at which the density is half of its peak value, and a is the diffuseness parameter.

For light nuclei from ^{7}Li to ^{16}O, the density corresponded to a harmonic-oscillator potential:

$$\rho_{p,n}(r) = \rho_{p,n}^0 \left[1 + \delta_{p,n}\left(\frac{r}{a_{p,n}^0}\right)^2\right] \exp\left[-\left(\frac{r}{a_{p,n}^0}\right)^2\right], \tag{5}$$

where $\delta_p = (Z-2)/3$, $\delta_n = (N-2)/3$, $a_{p,n}^o$ is the radial parameter. The quantity $\rho_{p,n}^o$ is found from the normalization condition ($\int \rho_{p,n}(r) d^3r = 1$).

In the calculation, the parameters of the proton distribution were assumed known and those of the neutron distribution were found from the comparison of the cross sections of the charge exchange scattering calculated using Eq. (3) with the experimentally measured ones in Ref. [1].

The cross sections calculated by Eq. (3) were fitted to the experimental data for the angles 4°, 7.5°, and 11.3°. For light nuclei up to oxygen we used the density distribution (5), and from the fit we found one parameter of the neutron density distribution, a_n°. This parameter is related to the rms neutron radius as

$$< r_n^2 >^{1/2} = a_n^0 (2.5 - 2/N)^{1/2}.$$

Table 1 shows the rms neutron radii found for the nuclei with $A \leq 16$ along with the proton rms radii used in the calculations.

Table 1
Parameters of the neutron distribution in light nuclei

Nucleus	a_n^o, fm	$< r_n^2 >^{1/2}$, fm	$< r_p^2 >^{1/2}$, fm	$< r_n^2 >^{1/2} - < r_p^2 >^{1/2}$, fm
^{7}Li	1.77(6)	2.51(8)	2.40	0.11(8)
^{9}Be	2.11(5)	3.06(7)	2.51	0.55(7)
^{10}B	1.73(4)	2.51(5)	2.45	0.06(5)
^{11}B	1.70(4)	2.51(5)	2.40	0.11(5)
^{12}C	1.75(3)	2.54(4)	2.45	0.12(4)
^{16}O	1.90(4)	2.85(6)	2.71	0.14(6)

We see that the neutron radius is considerably larger than the proton one in the case of ^{9}Be, possibly because the last unpaired neutron in ^{9}Be is at a significant distance from the core which is of the two α-particle structure.

For nuclei with $A \geq 19$, parametrization (4) was chosen for the density distribution. Since $d\sigma/d\Omega$ was measured only at three points, the two parameters (R_n and a_n) could not be determined simultaneously. Accordingly, one parameter was held constant and equal to the corresponding parameter of the proton distribution. In one series of calculations we took R_n constant ($R_n = R_p$) and in another we took a_n constant ($a_n = a_p$). Equally good descriptions of the experimental data were obtained in both series of calculations. For illustration, Fig. 3 compares the experimental values of $d\sigma/d\Omega$ with those calculated for the angle 7.5°. Also shown are the results calculated under the assumption of $\rho_n(r) = \rho_p(r)$.

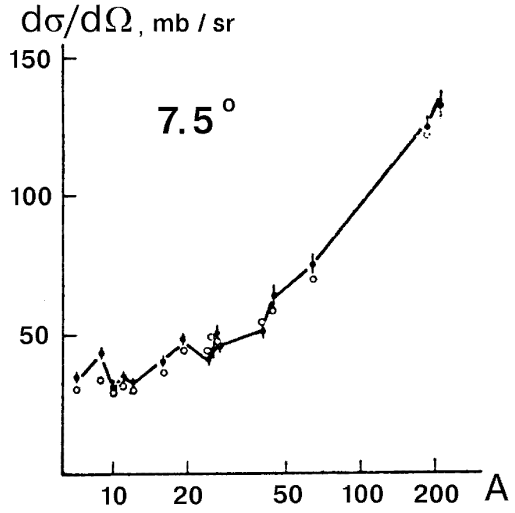

Fig. 3. Cross section for the charge exchange scattering. Solid circles – experimental data; open circles – calculations with $\rho_n(r) = \rho_p(r)$. The curve connects the calculated values which were obtained using the parameters of the neutron distribution determined in the present study).

Table 2 shows the parameters of the neutron distribution found from the two series of calculations.

Table 2
Parameters of the neutron distribution

Nucleus	a_n, fm	R_n, fm	$< r_n^2 >^{1/2}$, fm	$< r_n^2 >^{1/2} - < r_p^2 >^{1/2}$, fm
^{16}F	0.564	2.82(7)	3.03(4)	+0.13(4)
	0.61(2)	2.59	3.03(4)	+0.13(4)
^{24}Mg	0.538	2.73(10)	2.91(5)	-0.12(5)
	0.49(2)	2.94	2.92(5)	-0.11(5)
^{25}Mg	0.608	2.43(12)	2.94(6)	-0.17(6)
	0.55(2)	2.76	2.95(5)	-0.16(5)
^{26}Mg	0.524	3.17(10)	3.14(6)	+0.08(6)
	0.55(2)	3.05	3.13(6)	+0.07(6)
^{40}Ca	0.563	3.39(9)	3.36(6)	-0.07(6)
	0.54(2)	3.51	3.37(5)	-0.06(5)
^{44}Ca	0.549	3.73(11)	3.54(7)	+0.10(7)
	0.58(3)	3.58	3.52(6)	+0.08(6)
Cu*	0.569	4.40(5)	3.97(4)	+0.09(4)
	0.60(1)	4.20	3.95(4)	+0.07(4)
^{116}Sn	0.552	5.59(10)	4.79(7)	+0.12(7)
	0.52(3)	5.42	4.74(5)	+0.07(5)
^{124}Sn	0.534	5.80(10)	4.91(7)	+0.22(7)
	0.61(3)	5.49	4.82(5)	+0.13(5)
^{181}Ta	0.640	6.42(6)	5.51(5)	+0.03(5)
	0.65(2)	6.38	5.50(4)	+0.02(4)
Pb*	0.494	7.22(6)	5.89(5)	+0.39(5)
	0.64(2)	6.69	5.70(4)	+0.20(4)

* Natural isotopic mixture.

The errors of the neutron parameters (shown in parentheses) do not take into account the errors of the proton distribution parameters. This table shows the results of the two series of calculations, with the fixed $\alpha_n = \alpha_p$ and with the fixed $R_n = R_p$ (the parameter values given without errors were fixed).

For most of the nuclei, except for the heaviest, the rms neutron radii are nearly independent of the calculation procedure and can be considered as a reliable measure of the neutron distribution in these nuclei. To see how the rms neutron radii depend on the calculation procedure for the heavy nuclei, we carried out some further calculations with the fixed value $R_n = 0.9R_p$ and with the fixed value $a_n = 1.1a_p$. The rms neutron radius turned out to be very sensitive to the assumption on the value of the parameter R_n. For lead, for example, the calculations with the fixed value $R_n = 0.9R_p$ led to identical neutron and proton radii, although to reconcile the calculated results with the experimental data for this nucleus we had to increase the diffuseness parameter $a_n (a_n = 0.810$ fm) substantially above the proton value ($a_p = 0.494$ fm). Calculations with the fixed value $a_n = 1.1a_p$ caused essentially no change in the neutron radius in any of the nuclei.

It can thus be concluded that the experimental data presently available for heavy nuclei are not a sufficient basis for unambiguous determination of the rms neutron radii. We need more detailed measurements of $d\sigma/d\Omega$. The obtained information on the neutron distributions in such nuclei as ^{124}Sn and Pb may indicate that in these nuclei either the rms neutron radius is higher than the rms proton radius or the two are equal, with the diffuseness parameter being significantly bigger for the neutron distribution. For ^{181}Ta, the neutron and proton radii turned out to be nearly equal in different versions of calculations, possibly because ^{181}Ta has an unusually diffuse proton surface ($a_p = 0.64$ fm).

We have estimated the error in the rms neutron radii determination which is due to uncertainties in the parameters of the proton distribution and in the data on the nucleon-nucleon interaction. A change of σ_{eff}, by 0.5 mb for example, led to the change of the rms radius by ~ 0.04 fm in case of Pb. A change of the slope parameter for nucleon-nucleon elastic scattering by 0.5 $(\text{GeV/c})^{-2}$ changed the rms radius for Pb by $\sim$0.05 fm. And finally, when instead of the charge exchange data of G.Bizard et al. (1975) we used the data from the work of P.F.Shepard et al. (1969) (in which the neutron beam had a continuous energy distribution in the range 900–1200 MeV), the rms radius was changed by $\sim$ 0.2 fm. When we imposed the common normalization on the basis of ^{27}Al, all these errors were decreased substantially and their net effect on the rms neutron radius fell to no more than 0.05 fm. Changes in the parameters of the proton distribution within the experimental errors led to changes of the order of $\sim$ 0.05 fm in the rms neutron radii. In summary, possible errors in the experimental data used in the calculations lead to the error of $\sim$ 0.07 fm in the rms radii.

We also studied the stability of the results found for the rms neutron radii to variations in the nuclear density parametrization. For ^{40,44}Ca we carried out calculations with a three-parameter Fermi distribution, and for ^{116,124}Sn and Pb we used a three-parameter Gaussian distribution. Using different density parametrizations had no effect within the errors on the results found for the rms neutron radii.

Neutron production in pp and pd collisions

In 1 GeV proton interaction with hydrogen and deuterium, neutrons can be produced in the following reactions:

$$pp \to n\pi^+ p, \tag{6}$$

$$pd \to n\pi^+ p(n), \qquad pd \to n\pi^0 p(p), \tag{7}$$

$$pd \to np(p), \tag{8}$$

where the spectator nucleons in the deuteron are shown in parentheses.

Measurement of neutron spectra from reactions (6)–(7) is important for study of meson production in proton-proton and proton-neutron interactions.

Neutrons produced in reaction (8) at small angles appear due to the charge-exchange process $pn \to np$. Study of this process is especially important because the cross section for the reaction $pd \to n(pp)$ at the angle 0° is determined by the spin-dependent parts of the np charge-exchange amplitude. Thus, investigation of this process will permit one to obtain the information on the spin structure of the nucleon-nucleon amplitudes.

In Fig. 4 we show the double differential cross sections for production of neutrons in the energy range 350–1000 MeV from hydrogen and deuterium at angles of 4°, 7.5°, 11.3°, and 13.2°. Two well expressed peaks are visible in the spectra of neutron from deuterium. The peak in the high energy region is due to quasielastic knockout of neutrons. Identification of this peak as the quasielastic one is confirmed by the fact that in hydrogen (Fig. 4) this peak is absent (neutrons in hydrogen can be produced only in the inelastic process with production of π^+ mesons).

The peaks at energy near 600 MeV, which are observed both in hydrogen and in deuterium, are due to production of neutrons in inelastic reactions. The similarity of these peaks in shape and location is an indication of the fact that in *pd* collisions neutrons associated with the meson production are produced in quasifree *pp* or *pn* collisions. The location of the maxima of the peaks in hydrogen and deuterium in the missing mass spectrum M_x is in good agreement with the mass of the $\Delta(1232)$ resonance (the average value of M_x for all angles at the maxima of the spectra is 1230 ± 20 MeV/c^2). The width of the peak in hydrogen is M_x (FWHM)$=90 \pm 10$ MeV/c^2. In deuterium a broadening of the peak is observed, M_x (FWHM)$=130 \pm 20$ MeV/c^2, which may be due to the Fermi motion and due to the nucleon rescattering.

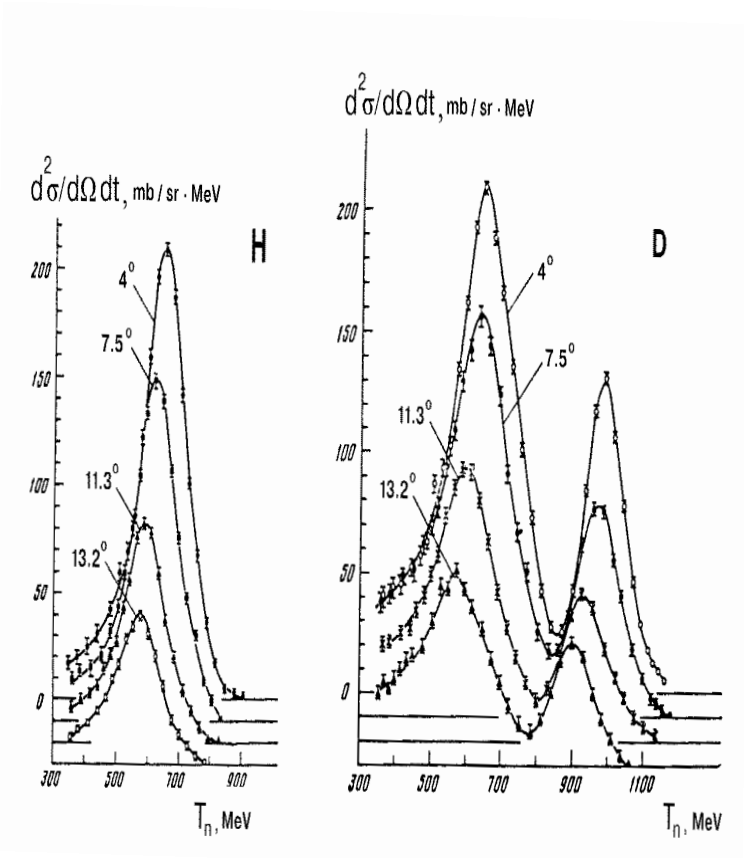

Fig. 4. Spectra of neutrons from hydrogen and deuterium. The statistical errors are shown. The curves are drawn by hand.

In Table 3 we give the cross sections for production of neutrons in reactions with the meson production $(d\sigma/d\Omega)^{\rm inel}$ integrated over the investigated energy range.

Table 3

Cross sections for production of neutrons with energy >350 MeV in inelastic processes

θ_n,	$(d\sigma/d\Omega)^{\rm inel}$, mb/sr		θ_n,	$(d\sigma/d\Omega)^{\rm inel}$, mb/sr	
deg.	H	D	deg.	H	D
4	42.7±3.4	52.1±4.2	11.3	20.7±1.7	29.6±2.4
7.5	31.0±2.5	44.7±3.6	13.2	14.0±1.1	20.4±1.6

If we assume that in the production of neutrons in reactions (6–7) the πN system has the isospin $I = 3/2$, then the ratio (A) of the inelastic cross sections in deuterium and in hydrogen should be equal to 4/3.

The difference of the A value from 4/3 gives an estimate of the contribution of the states with $I = 1/2$ to $(d\sigma/d\Omega)^{\rm inel}$. From our data this ratio, averaged over all angles, is close to 4/3 and equals to 1.39 ± 0.11. Thus, we can conclude that at the proton energy of 1 GeV the contribution of the states with $I = 1/2$ to the cross sections for reactions (6)–(7) is small and that the dominant process is the production of the $\Delta(1232)$ isobar in the intermediate state. It should be noted that the value of A, obtained from the data of C.W.Bjork et al. (1976) on the neutron production at the angle 0° from hydrogen and deuterium at the proton energies of 647 MeV and 800 MeV, is 1.72 ± 0.31 and 2.03 ± 0.36, respectively.

The obtained experimental results on the production of neutrons in reaction (8) and the data on the charge exchange in the elementary process $pn \to np$ provide the possibility of determining the contribution of the spin-dependent amplitude to the $pn \to np$ cross section at $t = 0$.

In the frame of the impulse approximation with the use of the property of completeness, the differential cross section for the charge exchange in the deuteron can be represented as follows:

$$\left(\frac{d\sigma}{dt}\right)_d = (1 - S(t))\left(\frac{d\sigma}{dt}\right)_1 + \left(1 - \frac{1}{3}S(t)\right)\left(\frac{d\sigma}{dt}\right)_2, \tag{9}$$

where $S(t)$ is the deuteron form factor, the quantities $(d\sigma/dt)_1$ and $(d\sigma/dt)_2$ are the spin-independent and spin-dependent parts of the cross section for the elementary charge exchange process $pn \to np$. It follows from Eq.(9) that in the impulse approximation for $t = 0\,[S(0) = 1]$ the differential cross section for the charge exchange in the deuteron is completely determined by the spin-dependent part of the pn charge exchange cross section:

$$\left(\frac{d\sigma}{dt}\right)_d\Big|_{t=0} = \frac{2}{3}\left(\frac{d\sigma}{dt}\right)_2\Big|_{t=0}. \tag{10}$$

This is explained in the following way. For $t = 0$ a system of two protons according to the Pauli principle can be found only in the state with the spin $J = 0$. Since in the initial state of the two nucleons (the deuteron) $J = 1$, the transition to the state with $J = 0$ can be accomplished (in the impulse approximation) only as a result of the interaction which depends on spin. Thus, extrapolating the value of the cross $(d\sigma/dt)_d$ to the point $t = 0$ we can determine the value of the spin-dependent part of the forward charge exchange amplitude. For the extrapolation, we chose an exponential t–dependence of the type $B \cdot \exp(bt)$. After fitting this expression to the data, we obtained

$$B = 21.4 \pm 2.0 \text{ mb/(GeV/c)}^2, \qquad b = 5.9 \pm 1.0 \text{ (GeV/c)}^{-2}.$$

In order to estimate the contribution of the spin-dependent part of the forward charge exchange amplitude, it is necessary to know the cross section $(d\sigma/dt)_p|_{t=0}$. In the experiment of G.Bizard et al. (1975), which was carried out at the energy of 1 GeV, this cross section is equal to $(d\sigma/dt)_p|_{t=0} = 50.8 \pm 1.2$ mb/(GeV/c)^2.

Using this cross section, we can obtain the contribution R of the spin-dependent part of the amplitude for $t = 0$ [4]:

$$R = \left(\frac{d\sigma}{dt}\right)_2 \Big/ \left(\frac{d\sigma}{dt}\right)_p = \frac{3}{2}\left(\frac{d\sigma}{dt}\right)_d \Big/ \left(\frac{d\sigma}{dt}\right)_p$$

$$R = 0.63 \pm 0.06. \qquad (11)$$

Conclusion

1. Calculations based on the Glauber diffraction theory have led to a good description of the experimental data on the charge exchange scattering of 1 GeV protons from nuclei ranging from Li to Pb at angles 4°, 7.5°, and 11.3°.

2. For most of the nuclei, the rms neutron radii turned out to be approximately equal to the proton ones. There were important differences in two cases:

   (a) ^{9}Be, for which the rms neutron radius is much larger than the rms proton radius;

   (b) Pb, for which the experimental data imply that either the rms neutron radius is larger than the proton one, or the diffuseness parameter for the neutron distribution is quite large.

3. The contribution of the spin-dependent part of the amplitude for $pn \to np$ forward charge exchange is equal to 0.63 ± 0.06.

References

[1] *V.N.Baturin, V.P.Koptev, E.M.Maev,* *M.M.Makarov*, *V.V.Neljubin, V.V.Sulimov, A.V.Khanzadeev, G.V.Shcherbakov.* Preprint PNPI–445, Gatchina, 1978. 39p. // Pis'ma Zh. Eksp. Teor. Fiz., 1979. V.30. P.86.

[2] *V.N.Baturin, V.P.Koptev, E.M.Maev,* *M.M.Makarov*, *V.V.Neljubin, V.V.Sulimov, A.V.Khanzadeev, G.V.Shcherbakov.* // Prib. Tekh. Eksp., 1979. No 4. P.47.

[3] *V.P.Koptev, E.M.Maev,* *M.M.Makarov*, *A.V.Khanzadeev.* // Yad. Fiz., 1980. V.31. P.1501.

[4] *V.N.Baturin, V.P.Koptev, E.M.Maev,* *M.M.Makarov*, *V.V.Neljubin, V.V.Sulimov, A.V.Khanzadeev, G.V.Shcherbakov.* // Yad. Fiz., 1980. V.31. P.396.